Crystal structures of self-assembled nanotubes from flexible macrocycles by weak interactions†

Romen Carrillo,[a] Matías López-Rodríguez,*[b] Víctor S. Martín[b] and Tomás Martín*[ab]

Received 20th January 2010, Accepted 7th May 2010
DOI: 10.1039/c001261k

Herein we report the crystal structures of tubular self-assemblies of flexible macrooligolides. The assembly is driven by the propensity of the macrocycles to create nearly flat structures displaying a void space within them and the cooperativity of weak directional interactions such as dipole–dipole interactions and CH···O hydrogen bonds and non-directional interactions such as van der Waals contacts. The significance of the stereochemistry and the size of the cavity in the formation of the nanotubes are also studied.

Introduction

The tubular structure is a very important kind of architecture in chemistry. Indeed natural nanotubes often display remarkable functions that have inspired a vast research on synthetic organic nanotubes either for a comprehensive study about the building processes or for the creation of simpler and tailored nanotubes.[1]

One of the most preferred strategies to accomplish a synthetic tubular structure is through self-assembly by stacking of macrocycles. Ring-shaped molecules of flat conformation as well as the right moieties arranged in a suitable way in the macrocycle employed are usually compulsory requirements for the induction of the cooperative action of weak bonds that leads to stable tubular complexes. Cyclic molecules may adopt or even intrinsically have a ring shape that generates a void space within them. That is the reason why self-assembled nanotubes are usually composed of macrocycles displaying not only moieties conferring rigidity such as multiple bonds and particularly aromatic rings, but also functional groups capable of generating a directional non-covalent interaction such as π-stacking and hydrogen bond interactions. Indeed, among the plethora of reported organic nanotubes, those built from macrocycles of such characteristics are majority: cyclic peptides,[2] calix[4]arenes,[3] cyclic oligomers of urea,[4] cyclodextrins,[5] cyclic oligosaccharides,[6] crown ethers[7] and cyclophanes[8] are common building blocks. However weak interactions, such as dipole–dipole and van der Waals interactions as far as we know, have never been used as the principal interactions to build a nanotube. Only recently, it has been described the formation of an organogel based on the self-assembling stacks of a boomerang-shaped molecule using dipole–dipole interactions in combination with π–π interactions.[9]

We have recently reported the synthesis of chiral cation receptors using 2-oxymethyl-3-oxy-tetrahydropyran as molecular scaffold and its use in host–guest chemistry[10] and as a model for the quantitative measurement of a CH-π interaction.[11] Although we expected that these molecules would be very flexible, in these previous works we realized that the backbone of these macrocycles seems to have inherent conformational preferences. Thus we decided to study the crystal structure of this kind of macrooligolides to check the influence of the stereochemistry of the tetrahydropyran (*cis* for compounds **1** and **2**, and *trans* for compounds **3** and **4**), and the size of the macrocycle on the formation of nanotubes (Scheme 1). We also studied their ability to stack by weak interactions, such as dipole–dipole, CH···O hydrogen bonds and van der Waals interactions.[12]

Results and discussion

Macrodiolides **1** and **3** were synthesized by a macrolactonization step from the appropriate hydroxy-acids. Additionally, along with the macrodiolides, the macrotetraolides **2** and **4** were obtained in the same reaction as the result of concomitant intermolecular esterification and macrolactonization (Scheme 2).[10] All compounds were characterized by standard

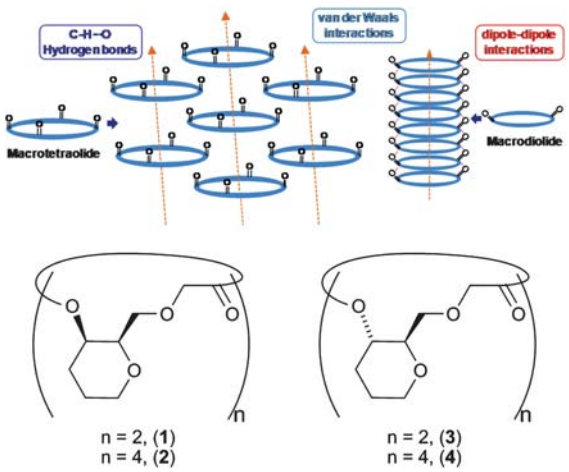

Scheme 1 Schematic representations of the self-assembled nanotubes. Structures of macrodiolides **1** and **3**, and macrotetraolides **2** and **4**.

[a]*Instituto de Productos Naturales y Agrobiología, CSIC, Avenida Astrofísico Francisco Sánchez, 3, 38206 La, Laguna, Tenerife, Spain. E-mail: tmartin@ipna.csic.es; Fax: (+34) 922-260-135; Tel: (+34) 922-260-190 ext. 250*
[b]*Instituto Universitario de Bio-Orgánica "Antonio González" Universidad de La Laguna, Avenida Astrofísico Francisco Sánchez, 2, 38206 La Laguna, Tenerife, Spain. E-mail: malopez@ull.es; Fax: (+34) 922-318-571; Tel: (+34) 922-318-588*

† CCDC reference numbers 266195, 266197, 266198 and 776407–776409. For crystallographic data in CIF or other electronic format see DOI: 10.1039/c001261k

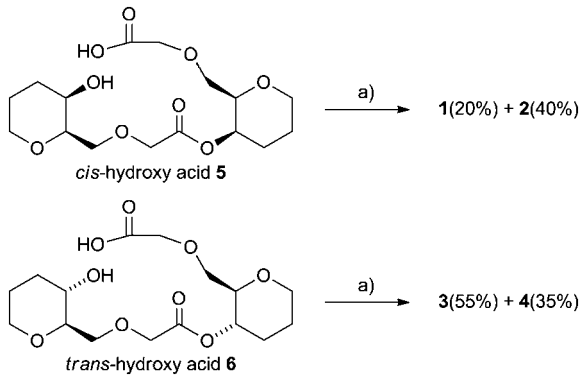

Scheme 2 Synthesis of the macrooligolides. Reagents and conditions: a) 2,4,6-trichlorobenzoyl chloride, Et_3N, DMAP, THF (0.01 M) → toluene (0.001 M), Δ.

spectroscopic techniques. Crystal structures were obtained for compounds **2**, **3** and **4** (Fig. 1 and Table 1). Unfortunately all attempts to crystallize compound **1** were not successful. The crystal structure of the macrotetraolide **2**, a 28 membered central cycle, shows that it is quite prone to display a ring-shaped molecule of flat conformation (Fig. 1). The X-ray analysis reveals a molecule with a pseudo-quaternary symmetry which displays a distance (Å) between H8B and H38B of 6.83, and 8.39 between H28B and H48B resulting in an area for the hollow of approximately 57 $Å^2$. The *cis*-tetrahydropyran rings are located in the corners of the rectangle, all of them with the same conformation in which the oxygen in position 3 is axial (Scheme 1). The 2-oxy-ester moieties are in the *anti* disposition (with a O–CH_2–CO–O torsion angle of 165–178°), setting the ester bond plane perpendicular to the main plane of the macrocycle. This conformation displays the four carbonyl oxygens on the same face of the macrocyclic ring. The tetrahydropyran rings are slightly tilted out of the plane of the macrocycle, with their oxygen atoms pointing to the opposite face of the carbonyl oxygens.

However the most interesting feature of the crystal structure emerged from the corresponding packing within the lattice: the *cis*-macrotetraolide unit is connected with six other units trough three intermolecular C–H···O hydrogen bonds: C22H···O1, C42H···O31 and one bifurcated which links C25HA with O41 and O44 at the same time (Fig. 2a, 3a and Table 2). In all three interactions the macrotetraolide acts, at the same time, as a donor (by means of H22, H42 and H25A) and as an acceptor (by means of O1, O31, O41 and O44), being generated in this way the six intermolecular interactions per unit. Two-dimensional layers, parallel to the *ac* plane are generated by means of the C42H···O31 (translation along [100]), C22H···O1 (translation along [001]) hydrogen bonds and van der Waals contacts between H3B···O21 (1 + *x*, *y*, *z*), H37B···O43 (−1 + *x*, *y*, *z*), H33B···O41 (*x*, *y*, 1 + *z*), and C8···O23 (*x*, *y*, −1 + *z*). This layers are further linked, along the *b* axis, into a three-dimensional network by two bifurcated C–H···O hydrogen bond interactions per unit, between the hydrogen H25A and the two oxygen atoms O41 and O44 (Fig. 3a). The macrocyclic rings are placed forming long channels along the diagonal between axes *a* and *c*. The extended structure reveals that each molecule of compound **2** stacks on top of two other units to form intertwining nanotubes directed towards the same direction. The edge of each nanotube is part of the wall of the two neighbouring nanotubes (Fig. 2). Also, these monomers are aligned parallel but off-centred. Each macrocycle is slightly shifted (0.79 Å) from the previous one and the stacks are tilted 4.5° off of perpendicular as measured by the

Table 1 Crystallographic data and details of measurements for compounds **2–4**

Compound	**2**	**3**	**4**
Chemical formula	$C_{32}H_{48}O_{16}$	$C_{16}H_{24}O_8$	$C_{32}H_{48}O_{16}$
Molecular weight	688.71	344.36	688.71
T/K	293	293	293
Crystal size/mm	0.45×0.3×0.3	0.4×0.35×0.3	0.4×0.3×0.25
Crystal system	Monoclinic	Monoclinic	Monoclinic
Space group	$P2_1$	*C*2	*C*2
Z	2	2	2
a/Å	9.052(2)	16.546(7)	18.443(7)
b/Å	27.546(6)	4.490(1)	7.313(5)
c/Å	9.808(3)	14.124(7)	15.038(6)
β (°)	115.28(2)	125.50(3)	122.19(5)
V/$Å^3$	2211.4(10)	854.2(6)	1716.5(15)
D_c/g cm^{-3}	1.034	1.339	1.333
X-Ray wavelength	0.71073	0.71073	0.71073
μ(Mo-K*α*)/mm^{-1}	0.083	0.107	0.107
θ_{min}/°	2.41	1.77	3.08
θ_{max} (°)	26.37	27.94	27.39
Reflns collected	4388	1113	2090
reflns $I > 4\sigma(I)$	2546	1020	1911
R_1 (observed)	0.0722	0.064	0.0389
wR_2 (all)	0.2218	0.1629	0.0940

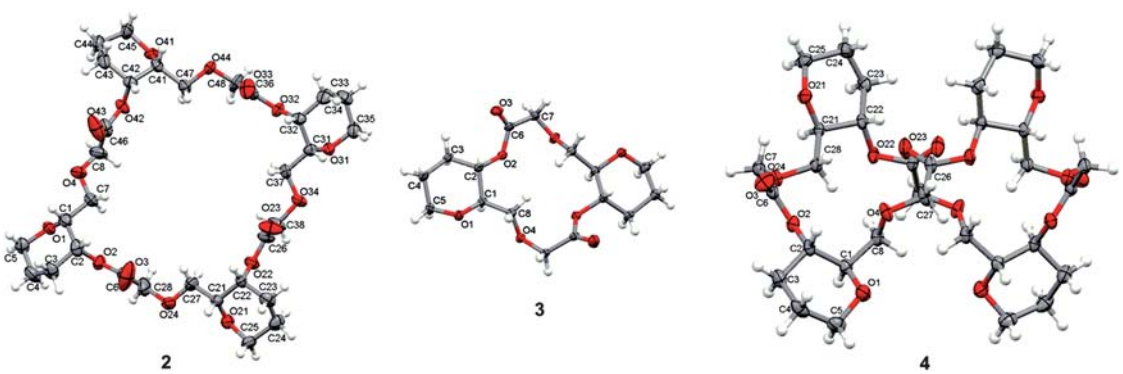

Fig. 1 Molecular structures of compounds **2**, **3** and **4** at 30% probability level.

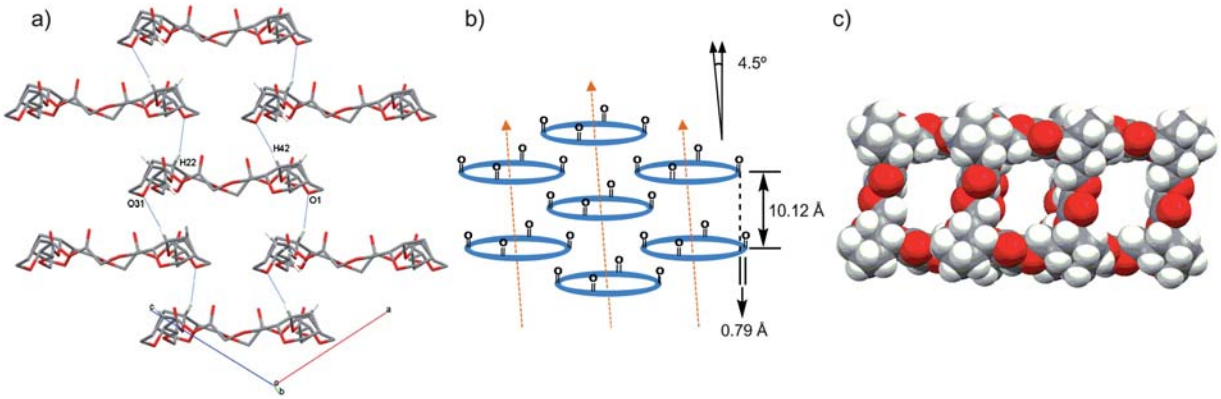

Fig. 2 a) Columnar packing of macrotetraolide **2**, showing the hydrogen atoms and oxygen atoms involved in CH···O hydrogen bonds (blue lines). b) Schematic representation of the columnar packing showing the intertwining nanotubes and several parameters. c) Upper view of the van der Waals cross-section of the hollow tubes along the diagonal between axes *a* and *c* (CPK model).

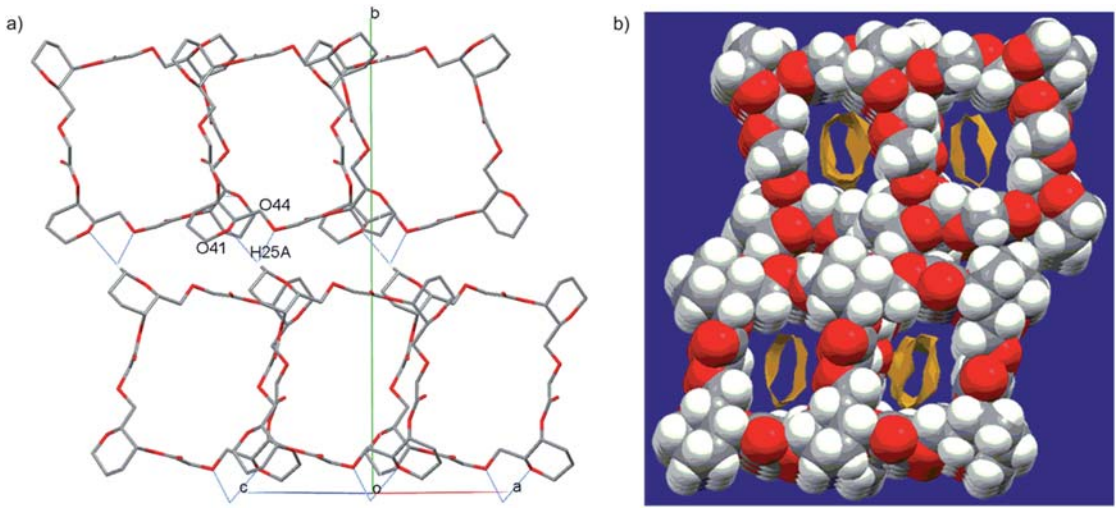

Fig. 3 a) Crystal packing of the nanotubular structure formed by macrotetraolide **2**, showing the hydrogen atoms and oxygen atoms involved in CH···O hydrogen bond (blue lines). b) Three dimensional packing arrangement of macrotetraolide **2**. Using a probe radius of 1.2 Å, the contact surfaces represent the infinite channels.

Table 2 Summary of intermolecular interactions (D–H···A; Å, °) operating in the crystal structures of compounds **2–4**

D···A	D–H	H···A	D···A	D-H···A	Symmetry operation
Compound **2**					
C22 H22 O1	0.98	2.54	3.388(8)	145	$x, y, 1 + z$
C25 H25A O41	0.97	2.59	3.401(11)	142	$-x, 1/2 + y, 1 - z$
C25 H25A O44	0.97	2.59	3.240(10)	124	$-x, 1/2 + y, 1 - z$
C42 H42 O31	0.98	2.51	3.448(7)	160	$1 + x, y, z$
Compound **3**					
C4 H4B O3	0.97	2.58	3.496(18)	157	$3/2 - x, 1/2 + y, 1 - z$
C7 H7A O1	0.97	2.53	3.458(18)	161	$-1/2 + x, 1/2 + y, z$
Compound **4**					
C27 H27B O1	0.97	2.52	3.224(5)	129	$3/2 - x, 1/2 + y, 1 - z$

inclination in the channel axis with respect to the normal of the macrocycle plane (Fig. 2b). The X-ray structure consists of an array of nanotubes in which each tubular stack is surrounded by four close neighbours, two of them arranged in the same direction and the other two in the opposite direction such that they cancel out their dipole moments (Fig. 3a). The packing coefficient of this crystal is around 52.3%. This value is smaller than those typical of organic crystals (66–77%)[13] and is in accordance with those obtained for some porous organic crystals. The inner surface of the nanotube is an irregular rectangle and its diameter can be estimated at approximately 4 Å (Fig. 3b).[14] The channels inside the tubes contain some electron density that should be associated with massively disordered solvent. Noteworthy, these nanotubes are built up only exclusively by weak intermolecular interactions such as CH···O hydrogen bonds and van der Waals contacts, indicating the great stability of the non-covalent organic framework.[15]

The stereochemistry of the tetrahydropyran unit is vital for the formation of the nanotube. Thus, the *trans*-macrotetraolide **4** does not crystallize as hollow tubes, but rather, a completely different structure is observed. In the X-ray of the *trans*-macrotetraolide **4**, the asymmetric unit is composed of only one half of the molecule; the full macrocycle is generated by means

of a crystallographic binary rotation axis. The molecule displays a twisted saddle-like structure (Fig. 1). This structure has arranged two of the *trans*-tetrahydropyrans in the stirrups position and the other two in the pommel and in the cantle. Also, the 2-oxy-ester moieties are present in *anti* and *syn* conformations (with a O–CH_2–CO–O torsion angle of −169° and −13°, respectively). The two carbonyl groups belonging to the *syn* 2-oxy-ester moieties are directed outward from the central macroring and the other two belonging to the *anti* 2-oxy-ester moieties are directed inward. The oxygen atoms of the latter are involved in van der Waals contacts with hydrogen atoms H22, helping to keep the centre ring collapsed and thus generating a folded structure. Additionally, in the crystal structure each asymmetric unit is connected with other two through a C–H···O hydrogen bond: C27HB···O1 (Fig. 4 and Table 2). In this interaction, the asymmetric unit acts, at the same time, as a donor (by means of H27B) and as an acceptor (by means of O1), being generated in this way the two intermolecular interactions. The other symmetric half of the molecule is engaged in a set of equivalent hydrogen bonds. As a result, each full macrocyclic molecule is associated with another four in a two-dimensional network of hydrogen bonds, parallel to the *bc* plane, generated by means of the C27HB···O1 hydrogen bonds (Fig. 4 and Table 2). These sheets are further linked, along the *c* axis, into a three-dimensional network by means of van der Waals contacts. The *trans*-macrotetraolide **4** units fit on top of each other, like stacked saddles, to form a columnar structure along the *b* axis. This is a consequence of the high complementarity between the top and bottom parts of the molecule along this axis (Fig. 5). The monomers are held together (along the *b* axis) by van der Waals contacts between H1···O21 (2 − *x*, −1 + *y*, 1 − *z*), H4B···O3 (*x*, −1 + *y*, *z*), H8A···H23B (*x*, −1 + *y*, *z*), and H27A···H24B (*x*, −1 + *y*, *z*). Also, the X-ray reveals a structure consisting of an array of columns in which each column is surrounded by four close neighbours, yet in this case the columns are displayed in parallel.

The relevance of the size of the macrocycle was also studied for the *trans*-isomers. The X-ray analysis of the macrodiolide **3**, a 14 membered central ring, reveals a *C*2 symmetry molecule with a practically flat structure (Fig. 1). The crystal structure of the macrodiolide **3** is quite similar to that of the *trans* macrotetrolide **4**. The main difference is that in the dimer **3** the oxygen atoms of the carbonyl groups participate in the hydrogen bonds. Thus, the asymmetric unit is only composed of one half of the molecule and the full macrocycle is generated by means of a crystallographic binary rotation axis. The *trans*-tetrahydropyran rings are located in the same plane of the central macrocycle, and with both substituents in equatorial position. The rectangular shaped cavity shows small dimensions. The hydrogen atoms H8A on C8

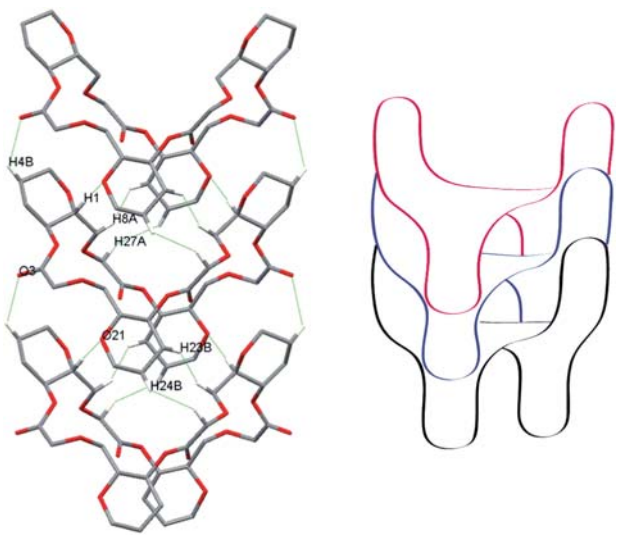

Fig. 5 Side view of the columnar structure formed by macrotetraolide **4**, showing the hydrogen atoms and oxygen atoms involved in van der Waals interactions (green lines). Schematic representation of stacked saddles.

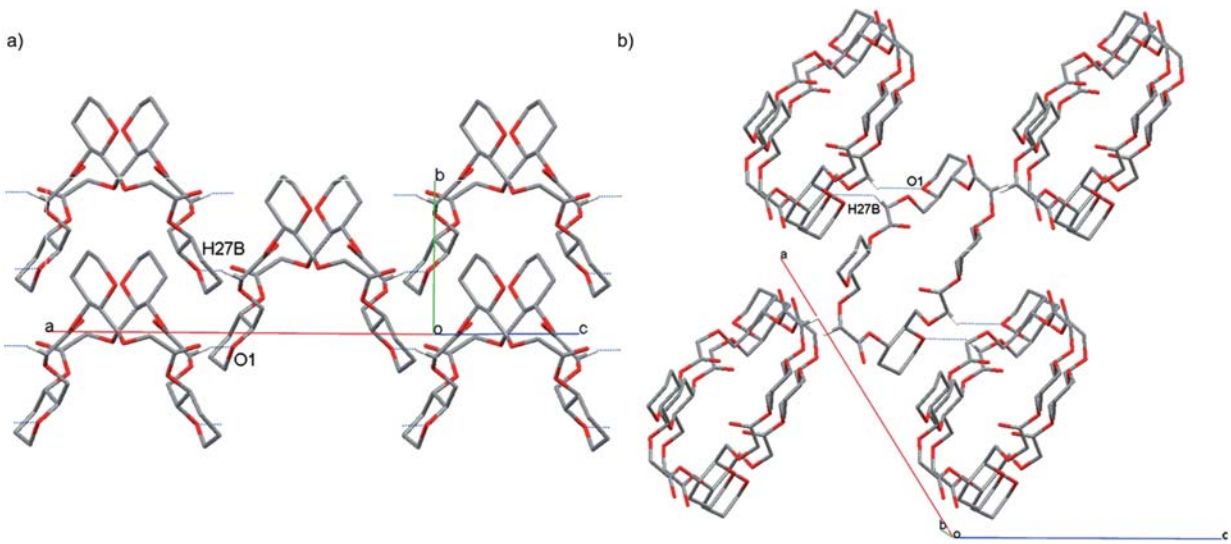

Fig. 4 a) Crystal packing of macrotetraolide **4** showing the hydrogen atoms and oxygen atoms involved in CH···O hydrogen bond (blue lines). b) Upper view of the columnar packing.

and C8A point inward, with an intramolecular H···H distance of 2.27 Å, filling most of the interior cavity. Additionally, the 2-oxy-ester moieties are in a *quasi-syn* disposition (with a O–CH_2-CO–O torsion angle of 25.1°), with both carbonyl groups directed to the same face of the macrocyclic ring, but with an inclination of 45° respect to the channel axis.

In the crystal structure, each asymmetric unit is connected with other four through two C–H···O hydrogen bonds: C4HB···O3 and C7HA···O1 (Table 2). In both interactions, the asymmetric unit acts, at the same time, as a donor (by means of H4B and H7A) and as an acceptor (by means of O3 and O1), being generated in this way the four intermolecular interactions. The other symmetric half of the molecule behaves in a similar way. As a result, each full macrocyclic molecule is associated with another eight in a three-dimensional network of C–H···O hydrogen bonds. In first place, two-dimensional hydrogen-bonding networks, parallel to the *bc* plane are generated by means of the C4HB···O3 hydrogen bonds and then the two-dimensional arrangements are further linked, along the *c* axis, into the three-dimensional network by means of the C7HA···O1 hydrogen bonds (Fig. 6a and Table 2). As it is shown in Fig. 7, a decrease in the cavity size of the macrocycle does not affect the tendency for stacking into nanotubes. In contrast, an infinite nanotube along the *b* axis is formed, although in this case the nanotube is capped

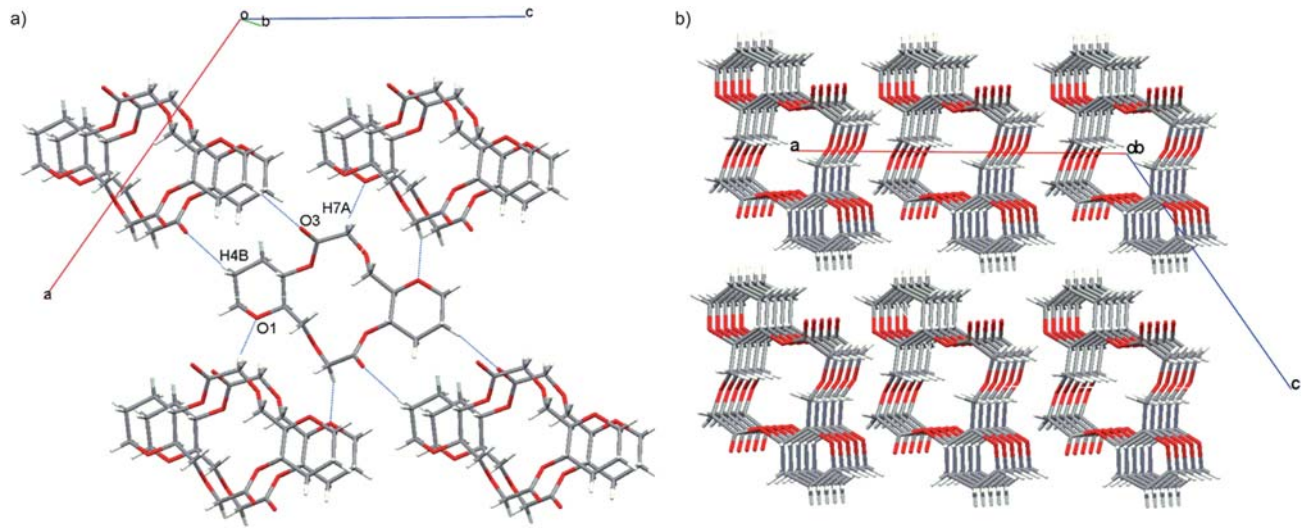

Fig. 6 a) Crystal packing of macrodiolide **3** showing the hydrogen atoms and oxygen atoms involved in CH···O hydrogen bond (blue lines). b) Upper view of the columnar packing.

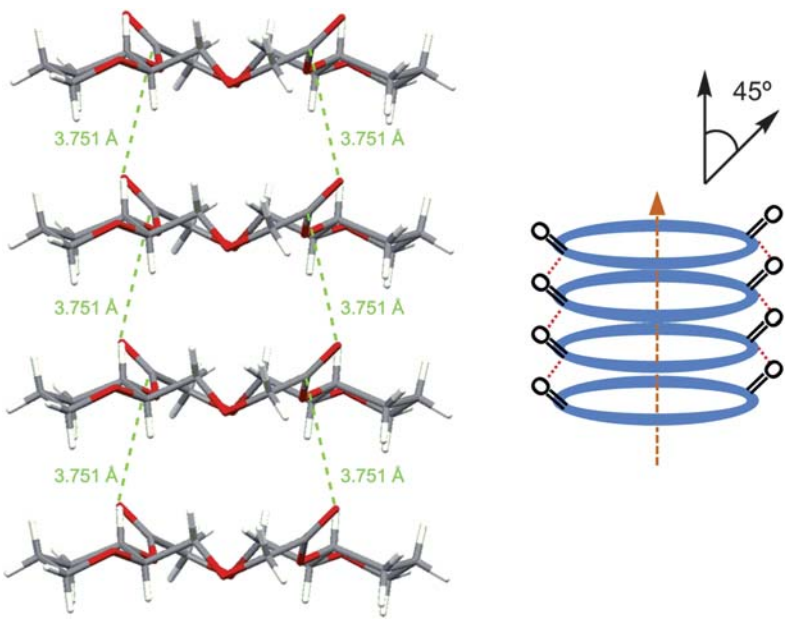

Fig. 7 Side view of the nanotubular structure formed by macrodiolide **3**. Schematic representation and the angle displayed between the channel axis and the carbonyl groups.

inside by the hydrogen atoms H8A. Flat ring-shaped macrodiolide monomers are held together (along the *b* axis) by backbone-backbone van der Waals contacts between the axial hydrogen atoms from the tetrahydropyran rings [H2···H3A (x, $-1 + y$, z), H1···H2 (x, $1 + y$, z) and H1···H8B ($2 - x$, $1 + y$, $2 - z$)] and carbonyl-carbonyl dipole interactions. The equivalent carbonyl groups are parallel, and the intermolecular distance between the carbonyl oxygen of one unit and the carbonyl carbon of the next unit is 3.751(9) Å. This distance is bigger than the sum of their van der Waals radii ($r_O + r_C \approx 3.15$ Å) and also the angle between the lone pair (n) of the carbonyl oxygen and the antibonding orbital (π^*) of the carbonyl carbon is unfavourable, therefore, an electronic delocalization through an $n \rightarrow \pi^*$ interaction, can be discarded.[16] However, this distance is in agreement with a carbonyl-carbonyl interaction in a parallel fashion of type III, according with the classification proposed by Allen,[17] where the proximity of the carbonyl groups produces a simple Coulombic attraction between the negatively polarized O and the positively C (Fig. 7).[18] These interactions can work in a positive cooperative way, making the assembling even more stable. Each macrodiolide is perpendicular to and centred on the crystallographic secondary axis in the crystal of **3**. The X-ray structure consists of an array of nanotubes in which each tubular stack is surrounded by four close neighbours. However, beyond all expectations, the crystal packing found shows all the nanotubes oriented in parallel in the same direction (Fig. 6b).

Taking into account the results obtained with macrotetraolide **2** and macrodiolide **3** in the formation of nanotubes, it seems extremely important the degree of inclination of the carbonyl groups with respect to the plane of the macrocycle, so that the carbonyl-carbonyl interactions play the key role to build up the nanotube. In macrotetraolide **2** this angle is around 87°, making very difficult the direct approach between the carbonyl oxygen atoms of one unit and the carbonyl carbon atoms of the next one due to the steric hindrance. However, in macrodiolide **3** this angle is 135° (or 45° respect to the *b* axis) allowing the approach between the carbonyls in a parallel fashion as shown in Fig. 7. Moreover, the value of this angle is optimal to maximize the van der Waals contacts between the backbones of the macrocycles, making the assembling even more stable.

Conclusions

In summary, there are two important factors for the tubular self-assembly to take place: the tendency of the macrocycle to display a void space and the existence of a net of molecular interactions oriented in a suitable way to allow the stacking. We have shown that weak interactions, such as backbone-backbone van der Waals contacts, carbonyl-carbonyl dipole interactions and C–H···O hydrogen bonds interactions can be used to build up nanotubes. The stereochemistry of the tetrahydropyran unit is vital, and whereas the *cis*-tetrahydropyran-tetramer **2** yields a set of intertwined nanotubes arranged antiparallely along the diagonal between axes *a* and *c*, the *trans*-tetrahydropyran-tetramer **4** yields a columnar structure along the *b* axis. However, the size of the macrocycle is not a determining factor and a smaller nanotube made from macrodiolide **3** is possible. In this case the nanotubes are displayed in parallel, and a cooperative carbonyl-carbonyl dipole interaction builds up the nanotube. Thus, apparently flexible macrocycles, lacking appropriate moieties to display strong directional interactions are able to yield *a priori* unexpected self-assembled nanotubes.

Experimental

All reagents were commercially available and used as received. ^{1}H NMR spectra were recorded on Brucker Advance spectrometers 400 and 300 at 400 and 300 MHz, respectively; ^{13}C NMR spectra were recorded at 75 MHz, and chemical shifts are reported relative to internal Me_4Si. Infrared spectra were obtained in KBr disks on a Bruker IFS 55 FTIR spectrometer in the range of 4000 − 600 cm^{-1}. Elemental analyses of C, H, and N were determined with a Fisons EA 1108 CHNS–O elemental analyzer. HRMS data were recorded using a Fisons instruments VG Autospec. Optical rotations were determined for solutions in chloroform. Column chromatography was performed on silica gel, 60 Å and 0.2–0.5 mm and Sephadex LH-20. Compounds were visualized by use of UV light, 2.5% phosphomolybdic acid in ethanol or vanillin with acetic and sulfuric acid in ethanol with heating. All solvents were purified by standard techniques. Reactions requiring anhydrous conditions were performed under nitrogen. Anhydrous magnesium sulfate was used for drying solutions.

Synthesis

Preparation of the macrodiolide 1 and macrotetraolide 2. To a solution of the *cis*-hydroxy acid **5**[10] (27 mg, 0.07 mmol) in dry THF (6.13 mL, 0.012 M) at room temperature, were added Et_3N (20 μL, 0.15 mmol) and 2,4,6-trichlorobenzoyl chloride (15 μL, 0.1 mmol). After 2 h, the mixture was diluted with dry toluene (61 mL, 0.0012 M) and added slowly over DMAP (90 mg, 0.7 mmol) in boiling toluene (12 mL). The mixture was stirred at reflux for 1h. The solvent was evaporated and the residue purified by size exclusion chromatography (Sephadex LH-20 and MeOH as the mobile phase) to yield the macrodiolide **1** (5.1 mg, 20% yield) as an oil, and the macrotetraolide **2** (10.1 mg, 40% yield) as a white solid and oligomers (10 mg). Macrodiolide **1**: $[\alpha]_D^{25} = -31.2$ (*c* 0.33, $CHCl_3$); ^{1}H NMR ($CDCl_3$) δ 1.41 (d, $J = 12.6$ Hz, 2H), 1.68 − 1.77 (m, 2H), 1.85 − 1.97 (m, 2H), 2.10 (d, $J = 14.2$ Hz, 2H), 3.50 (ddd, $J = 1.8, 1.8, 11.8$ Hz, 2H), 3.62 (dd, $J = 5.4, 5.4$Hz, 2H), 3.67 − 3.77 (m, 4H), 4.05 (d, $J = 14.2$ Hz, 4H), 4.16 (d, $J = 14.3$ Hz, 2H), 5.08 (s, 2H); ^{13}C NMR ($CDCl_3$) δ 20.6 (t), 27.2 (t), 68.1 (t), 68.2 (d), 70.4 (t), 70.8 (t), 76.2 (d), 169.4 (s); IR (film) (cm^{-1}): 2928, 2854, 1736, 1217, 1095; MS (FAB) *m*/*z* (relative intensity): 367 (M + Na)$^+$ (19), 135 (8), 81 (51), 69 (100); HRMS (FAB) calcd for $C_{16}H_{24}O_8Na$ (M + Na)$^+$: 367.1369, found: 367.1387. Macrotetraolide **2**: mp 135 − 139 °C; $[\alpha]_D^{25} = -42.7$ (*c* 1.4, $CHCl_3$); ^{1}H NMR ($CDCl_3$) δ 1.40 (d, $J = 13.0$ Hz, 4H), 1.57 − 1.92 (m, 8H), 2.06 (d, $J = 13.4$ Hz, 4H), 3.32 − 3.68 (m, 12H), 3.99 (m, 4H), 4.05 (d, $J = 16.8$ Hz, 4H), 4.21 (d, $J = 16.8$ Hz, 4H), 5.01 (s, 4H); ^{13}C NMR ($CDCl_3$) δ 20.5 (t), 27.6 (t), 68.0 (d), 68.2 (t), 71.4 (t), 77.2 (d), 169.8 (s); IR (film) (cm^{-1}): 2954, 2855, 2362, 1751, 1437, 1202, 1132, 1094; MS (FAB) *m*/*z* (relative intensity): 711 (M + Na)$^+$ (8), 367 (5), 173 (16), 97 (100), 69 (17); HRMS (FAB): calcd for $C_{32}H_{48}O_{16}Na$ (M + Na)$^+$: 711.2840, found: 711.2793.

Preparation of the macrodiolide 3 and macrotetraolide 4. The same procedure used above to obtain compounds **1** and **2** was applied to *trans*-hydroxy acid **6**[10] on a 50 mg (0.11 mmol) scale, yielding macrodiolide **3** (19 mg, 55% yield) as a white solid and macrotetraolide **4** (12 mg, 35% yield) as a white solid: Macrodiolide **3**: mp 108 − 111 °C; $[\alpha]_D^{25} = +44.1$ (c 1.4, $CHCl_3$); ^1H NMR (δ, $CDCl_3$): 1.18–1.23 (m, 1H), 1.45–1.75 (m, 6H), 2.26 − 2.31 (m, 1H), 3.41 (ddd, $J = 3.1$, 11.4, 11.4 Hz, 1H), 3.48–3.68 (m, 3H), 3.93–3.98 (m, 2H), 4.29 (d, $J = 16.9$, 1H), 4.50 (ddd, $J = 4.9$, 10.3, 10.3 Hz, 1H); ^{13}C NMR (δ, $CDCl_3$): 24.6 (t), 29.1 (t), 67.6 (t), 68.8 (t), 69.3 (d), 71.9 (t), 78.7 (d), 169.6 (s); IR (film)(cm^{-1}): 2949, 2863, 1734, 1261; MS (FAB) *m*/*z* (relative intensity): 367 $(M + Na)^+$ (7), 345 $(M + H)^+$ (30), 307(14), 173 (31), 97 (93); HRMS (FAB): calcd for $C_{16}H_{25}O_8$ $(M + H)^+$: 345.1549, found: 345.1558. Macrotetraolide **4**: mp 152–155 °C; $[\alpha]_D^{25} = +28.2$ (c 1.3, $CHCl_3$); ^1H NMR (δ, $CDCl_3$): 1.48 (dddd, $J = 4.6$, 12.0, 12.0, 12.0 Hz, 4H), 1.68–1.80 (m, 8H), 2.16–2.20 (m, 4H), 3.34–3.46 (m, 8H), 3.54 (dd, $J = 6.0$, 10.0 Hz, 4H), 3.73 (d, $J = 10.0$ Hz, 4H), 3.95 (d, $J = 10.6$ Hz, 4H), 4.11 (dd, $J = 17.0$, 17.0 Hz, 8H), 4.76 (ddd, $J = 4.7$, 10.4, 10.4 Hz, 4H); ^{13}C NMR (δ, $CDCl_3$): 24.8 (t), 29.1 (t), 67.7 (t), 68.6 (t), 68.7 (d), 71.5 (t), 78.7 (t), 169.5; IR (film)(cm^{-1}): 2949, 2857, 1753, 1456; MS (FAB) *m*/*z* (relative intensity): 711 $(M + Na)^+$ (66), 689 $(M + H)^+$ (11), 173 (14), 136 (39), 97 (100), 73 (28); HRMS (FAB): calcd for $C_{32}H_{49}O_{16}$ $(M + H)^+$: 689.3021, found: 689.2986.

Crystals of all compounds were grown under identical conditions, from a solution of the macrooligolide in dichloromethane by vapor-phase equilibration with *n*hexane.

Crystal structure determination

The structure was solved by direct methods using SIR97.[19] Refinement was performed with SHELXL-97[20] using full-matrix least squares with anisotropic thermal parameters for all non-H atoms. The hydrogen atoms were placed at idealized positions. Data reduction and cell parameters refinement for the macrotetrolides **2** and **4**, and for macrodiolide **3** were carried out with the programs COLLECT[21] and DENZO.[22] The absolute structures were established based on chemical grounds.

Acknowledgements

The authors thank Dr David Tejedor for helpful discussions. This research was supported by the Spanish MICINN-FEDER (CTQ2008-03334/BQU, CTQ2008-06806-C02-01/BQU and CTQ2008-06754-C04-01/PPQ), the MSC (RTICC RD06/0020/1046) and the Canary Islands FUNCIS (PI 01/06).

References

1 D. T. Bong, T. D. Clark, J. R. Granja and M. R. Ghadiri, *Angew. Chem. Int. Ed.*, 2001, **40**, 988.

2 (*a*) M. R. Ghadiri, J. R. Granja, R. A. Milligan, D. E. McRee and N. Khazanovich, *Nature*, 1993, **366**, 324; (*b*) M. R. Ghadiri, J. R. Granja and L. K. Buehler, *Nature*, 1994, **369**, 301; (*c*) K. Motesharei and M. R. Ghadiri, *J. Am. Chem. Soc.*, 1997, **119**, 11306; (*d*) J. Sánchez-Quesada, H. S. Kim and M. R. Ghadiri, *Angew. Chem., Int. Ed*, 2001, **40**, 2503; (*e*) S. Fernández-López, H. S. Kim, E. C. Choi, M. Delgado, J. Granja, A. Khasanov, K. Kraehenbuehl, G. Long, D. A. Weinberger, K. Wilcoxen and M. R. Ghadiri, *Nature*, 2001, **412**, 452; (*f*) D. Gauthier, P. Baillargeon, M. Drouin and Y. L. Dory, *Angew. Chem., Int. Ed*, 2001, **40**, 4635; (*g*) R. J. Brea and J. R. Granja, Self-Assembly of Cyclic Peptides in Hydrogen-Bonded Nanotubes, in *Dekker Encyclopedia of Nanoscience and Nanotechnology*, ed. J. A. Schwarz, C. I. Contescu and K. Putyera, Marcel Dekker, New York, 2004, p. 3439; (*h*) W. S. Horne, C. M. Wiethoff, C. Cui, K. M. Wilcoxen, M. Amorín, M. R. Ghadiri and G. R. Nemerow, *Bioorg. Med. Chem.*, 2005, **13**, 5145; (*i*) R. J. Brea, L. Castedo and J. R. Granja, *Chem. Commun.*, 2007, 3267; (*j*) P. Baillargeon, S. Bernard, D. Gauthier, R. Skouta and Y. L. Dory, *Chem. Eur. J.*, 2007, **13**, 9223; (*k*) I. Alfonso, M. Bolte, M. Bru, M. I. Burguete and S. V. Luis, *CrystEngComm*, 2009, **11**, 735.

3 (*a*) L. Baldini, F. Sansone, A. Casnati, F. Ugozzoli and R. Ungaro, *Journal of Supramolecular Chemistry*, 2002, **2**, 219; (*b*) L. J. Barbour and A. Jerga, *Science*, 2002, **296**, 2367; (*c*) V. G. Organo, A. V. Leontiev, V. Sgarlata, H. R. Rasika Dias and D. M. Rudkevich, *Angew. Chem. Int. Ed.*, 2005, **44**, 3043; (*d*) S. J. Dalgarno, G. W. V. Cave and J. L. Atwood, *Angew. Chem. Int. Ed.*, 2006, **45**, 570; (*e*) A. N. Lazar, N. Dupont, A. Navaza and A. W. Coleman, *Chem. Commun.*, 2006, 1076; (*f*) A. Casnati, R. Liantonio, P. Metrangolo, G. Resnati, R. Ungaro and F. Ugozzoli, *Angew. Chem. Int. Ed.*, 2006, **45**, 1915; (*g*) L. Baldini, F. Sansone, C. Massera, A. Casnati, F. Ugozzoli and R. Ungaro, *Inorganica Chimica Acta*, 2007, **360**, 970; (*h*) S. J. Dalgarno, P. K. Thallapally, L. J. Barbour and J. L. Atwood, *Chem. Soc. Rev.*, 2007, **36**, 236; (*i*) P. K. Thallapally, B. P. McGrail, J. L. Atwood, C. Gaeta, C. Tedesco and P. Neri, *Chem. Mat*, 2007, **19**, 3355.

4 (*a*) L. S. Shimizu, M. D. Smith, A. D. Hughes and K. D. Shimizu, *Chem. Commun.*, 2001, 1592; (*b*) V. Semetey, C. Didierjean, J.-P. Briand, A. Aubry and G. Guichard, *Angew. Chem. Int. Ed*, 2002, **41**, 1895; (*c*) L. S. Shimizu, A. D. Hughes, M. D. Smith, M. J. Davis, B. P. Zhang, H.-C. zur Loye and K. D. Shimizu, *J. Am. Chem. Soc.*, 2003, **125**, 14972; (*d*) L. Fisher, M. Decossas, J.-P. Briand, C. Didierjean and G. Guichard, *Angew. Chem. Int. Ed*, 2009, **48**, 1625; (*e*) J. L. López, E. M. Pérez, P. M. Viruela, R. Viruela, E. Ortí and N. Martín, *Org. Lett.*, 2009, **11**, 4524.

5 (*a*) A. Harada, J. Li and M. Kamachi, *Nature*, 1992, **356**, 325; (*b*) A. Harada, J. Li and M. Kamachi, *Nature*, 1993, **364**, 516; (*c*) G. Li and L. B. McGown, *Science*, 1994, **264**, 249.

6 (*a*) P. R. Ashton, C. L. Brown, S. Menzer, S. A. Nepogodiev, J. F. Stoddart and D. J. Williams, *Chem. Eur. J.*, 1996, **2**, 580; (*b*) P. R. Ashton, S. J. Cantrill, G. Gattuso, S. Menzer, S. A. Nepogodiev, A. N. Shipway, J. F. Stoddart and D. J. Williams, *Chem. Eur. J.*, 1997, **3**, 1299; (*c*) G. Gattuso, S. Menzer, S. A. Nepogodiev, J. F. Stoddart and D. J. Williams, *Angew. Chem. Int. Ed*, 1997, **36**, 1451.

7 (*a*) L. Kloo, P. H. Svensson and M. J. Taylor, *J. Chem. Soc., Dalton Trans.*, 2000, 1061; (*b*) K. M. Fromm and R. D. Bergougnant, *Solid State Sci.*, 2007, **9**, 580.

8 C. Dawson, P. N. Horton, M. B. Hursthouse and S. L. James, *CrystEngComm*, 2010, **12**, 1048.

9 I. Hisaki, H. Shigemitsu, Y. Sakamoto, Y. Hasegawa, Y. Okajima, K. Nakano, N. Tohnai and M. Miyata, *Angew. Chem. Int. Ed.*, 2009, **48**, 5465.

10 (*a*) R. Carrillo, V. S. Martín and T. Martín, *Tetrahedron Lett.*, 2004, **45**, 5215; (*b*) R. Carrillo, V. S. Martín, M. López-Rodríguez and T. Martín, *Tetrahedron*, 2005, **61**, 8177.

11 R. Carrillo, V. S. Martín, M. López-Rodríguez and T. Martín, *Angew. Chem. Int. Ed.*, 2009, **48**, 7803.

12 (*a*) G. R. Desiraju, *Crystal Engineering. The Design of Organic Solids*, Elsevier, Amsterdam, 1989; (*b*) T. Steiner, *Chem. Commun.*, 1997, 727; (*c*) G. R. Desiraju, *Acc. Chem. Res.*, 2002, **35**, 565; (*d*) K. Biradha, *CrystEngComm*, 2003, **5**, 374.

13 (*a*) A. I. Kitaigorodskii, *Molecular Crystals and Molecules*, Academic Press, New York, 1973; (*b*) See ref. 10 (a); (*c*) A. Gavezzotti, *Acc. Chem. Res.*, 1994, **27**, 309; (*d*) K. Nakano, K. Sada, Y. Kurozumi and M. Miyata, *Chem. Eur. J.*, 2001, **7**, 209.

14 A spherical probe with a 2 Å radius can roll perfectly along the interior surface of the channel.

15 For some examples of non-covalent organic porous, see:(*a*) D. V. Soldatov, I. L. Moudrakovski and J. A. Ripmeester, *Angew. Chem. Int. Ed.*, 2004, **43**, 6308; (*b*) D. V. Soldatov, I. L. Moudrakovski, E. V. Grachev and J. A. Ripmeester, *J. Am. Chem. Soc.*, 2006, **128**, 6737; (*c*) L. J. Barbour, *Chem. Commun.*, 2006, 1163; (*d*) M. B. Dewal, M. W. Lufaso, A. D. Hughes,

S. A. Samuel, P. Pellechia and L. S. Shimizu, *Chem. Mater.*, 2006, **18**, 4855; (*e*) S. J. Dalgarno, P. K. Thallapally, L. J. Barbour and J. L. Atwood, *Chem. Soc. Rev.*, 2007, **36**, 236; (*f*) T. Tozawa, J. T. A. Jones, S. I. Swamy, S. Jiang, D. J. Adams, S. Shakespeare, R. Clowes, D. Bradshaw, T. Hasell, S. Y. Chong, C. Tang, S. Thompson, J. Parker, A. Trewin, J. Bacsa, A. M. Z. Slawin, A. Steiner and A. I. Cooper, *Nature Materials*, 2009, **8**, 973.

16 (*a*) L. E. Bretscher, C. L. Jenkins, K. M. Taylor, M. L. DeRider and R. T. Raines, *J. Am. Chem. Soc.*, 2001, **123**, 777; (*b*) M. L. DeRider, S. J. Wilkens, M. J. Waddell, L. E. Bretscher, F. Weinhold, R. T. Raines and J. L. Markley, *J. Am. Chem. Soc.*, 2002, **124**, 2497; (*c*) B. C. Gorske, B. L. Bastian, G. D. Geske and H. E. Blackwell, *J. Am. Chem. Soc.*, 2007, **129**, 8928; (*d*) A. Choudhary, D. Gandla, G. R. Krow and R. T. Raines, *J. Am. Chem. Soc.*, 2009, **131**, 7244.

17 (*a*) A. Gavezzotti, *J. Phys. Chem.*, 1990, **94**, 4319; (*b*) F. H. Allen, C. A. Baalham, J. P. M. Lommerse and P. R. Raithby, *Acta Cryst.*, 1998, **B54**, 320.

18 For recent examples on the use of dipole–dipole interactions to promote self-assembly, see:(*a*) Y. Li, M. Pink, J. A. Karty and A. H. Flood, *J. Am. Chem. Soc.*, 2008, **130**, 17293; (*b*) M. del C. Rivera-Sánchez, I. Andújar-de-Sanctis, M. García-Arriaga, V. Gubala, G. Hobley and J. M. Rivera, *J. Am. Chem. Soc.*, 2009, **131**, 10403.

19 A. Altomare, M. C. Burla, M. Camalli, G. Cascarano, C. Giacovazzo and A. R. Guagliardi, *J. Appl. Crystallogr.*, 1999, **32**, 115.

20 G. M. Sheldrick, *SHELXL-97 Program for the Refinement of Crystal Structures*; University of Göttingen: Göttingen, Germany, 1997.

21 *Nonius Kappa CCD Server Software*; R. V. Nonius, Delft, The Netherlands, 1998.

22 (*a*) Z. Otwinowsky and W. Minor, In *Methods in Enymology, Macromolecular Crystallography Part A*; (*b*) C. E. Carter and R. M. Sweet, ed.; Academic Press; *University of Texas, Southwestern Medical Center at Dallas*, 1997, 276, p. 307.